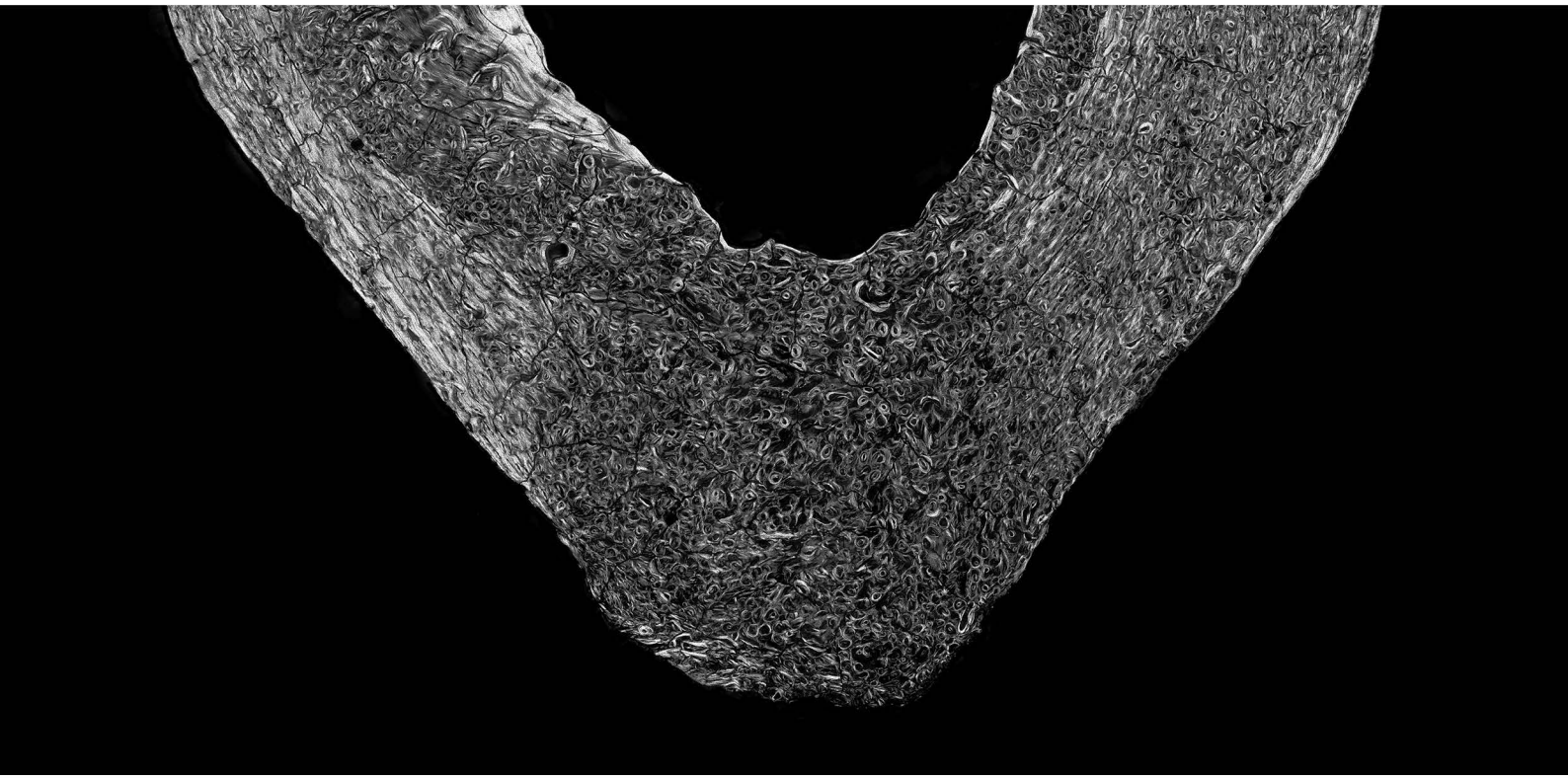

Timothy G. Bromage
Yusuf M. Juwayeyic
Julia A. Katris
Santiago Gomez
Olexandra Ovsiya
Justin Goldsteine
Malvin N. Janalf
Bin Hua
Friedemann Schrenk

The scaling of human osteocyte lacuna density with body size and metabolism

Comptes rendus Palevol

C. R. Palevol 15 (2016) 33–40

Contents lists available at ScienceDirect

Comptes Rendus Palevol

www.sciencedirect.com

Human Palaeontology and Prehistory (Physical Anthropology)

The scaling of human osteocyte lacuna density with body size and metabolism

Gamme de densité de lacunes d'ostéocyte chez l'homme en fonction de la taille corporelle et du métabolisme

Timothy G. Bromage [a,*,b], Yusuf M. Juwayeyi [c], Julia A. Katris [a], Santiago Gomez [d], Olexandra Ovsiy [a], Justin Goldstein [e], Malvin N. Janal [f], Bin Hu [a], Friedemann Schrenk [b]

[a] *Departments of Biomaterials & Biomimetics and Basic Science & Craniofacial Biology, New York University College of Dentistry, 345 East 24th Street, 10010 New York, USA*
[b] *Department of Palaeoanthropology, Senckenberg Research Institute Frankfurt a.M., Senckenberganlage 25, 60325 Frankfurt am Main, Germany*
[c] *Department of Sociology/Anthropology, Long Island University, 1 University Plaza, Brooklyn, 11201 New York, USA*
[d] *Department of Anatomy and Pathology, University of Cádiz, Fragela 9, 11003 Cádiz, Spain*
[e] *Department of Anthropology, Columbia University, 452 Schermerhorn Extension, 1200, Amsterdam Avenue, 10027 New York, USA*
[f] *Department of Epidemiology and Health Promotion, New York University College of Dentistry, 380, Second Avenue, 10010 New York, USA*

ARTICLE INFO

Article history:
Received 28 November 2014
Accepted after revision 12 September 2015
Available online 4 November 2015

Handled by Michel Laurin

Keywords:
Osteocyte lacunae density
Cell proliferation
Body size
Metabolism
Havers-Halberg Oscillation
Multidien rhythm

ABSTRACT

The aim of our research is to document osteocyte lacuna density (OCD) and its biological significance among humans of known life history. Twelve human midshaft femurs obtained from sub-Saharan Africans (Malawi) of Bantu origin and known life history were prepared for backscattered electron microscopy in the scanning electron microscope (BSE-SEM). Lacunae have a characteristic size and aspect ratio in BSE-SEM images that allowed them to be identified and automatically enumerated relative to the detected bone area in all of the images processed; values for adult whole femoral midshaft cross sections averaged about 100,000 osteocyte lacunae. Statistical tests reveal significant relationships between both OCD and osteocyte lacuna area with body height. It appears that the same increase in energetic efficiency observed in interspecific comparisons of the mass specific metabolic rate of bone at larger body sizes also characterizes body size categories among humans. Long period biological rhythms that regulate rates of cell proliferation explain some aspects of human body size variability.

Mots clés :
Densité de lacunes d'ostéocyte
Prolifération cellulaire

RÉSUMÉ

Le but de notre recherche est de documenter la densité de lacunes d'ostéocyte (OCD) et sa signification chez des Hommes à histoire de vie connue. Douze diaphyses de fémurs humains provenant d'Africains sub-sahariens (Malawi) d'origine bantoue et d'histoire de

* Corresponding author.
E-mail address: tim.bromage@nyu.edu (T.G. Bromage).

http://dx.doi.org/10.1016/j.crpv.2015.09.001
1631-0683/

Taille corporelle
Métabolisme
Oscillation Havers-Halberg
Rythme « multidien » (multijournalier)

vie connue ont été préparées pour examen au microscope à électrons rétrodiffusés en microscopie électronique à balayage (BSE-SEM). Les lacunes ont un rapport taille-aspect caractéristique sur les images BSE-SEM, ce qui permet de les identifier et de les dénombrer automatiquement en fonction de la zone osseuse détectée sur toutes les images analysées; les valeurs, dans les sections de diaphyse fémorale complète d'adulte, sont en moyenne de 100 000 lacunes d'ostéocyte. Des tests statistiques révèlent des relations significatives entre l'OCD et la surface des lacunes d'ostéocyte, d'une part, et la taille corporelle, d'autre part. Il apparaît que la même augmentation de puissance énergétique, observée dans les comparaisons inter-spécifiques du taux de masse métabolique de l'os, pour des tailles corporelles plus grandes, caractérise aussi des catégories de taille corporelle chez l'Homme. Les rythmes biologiques à période longue qui régulent les taux de prolifération expliquent certains aspects de la variabilité de taille du corps humain.

1. Introduction

Research on the chronobiology of mammalian mineralized tissues has provided evidence for a many-days "multidien"[1] metabolic rhythm that regulates body mass, which in turn manifests the life history continuum (Bromage et al., 2009, 2012). In enamel, the length of this rhythm is equal to the duration of time between one stria of Retzius to the next, the repeat period, and in bone it is the duration of time to form one lamella. This rhythm, called the Havers-Halberg Oscillation (HHO), is argued to regulate body mass by means of varying rates of cell proliferation and thus the cumulative growth of all major tissue and organ masses (Bromage and Janal, 2014). However, to date, this research has not included the growth of bone mass, nor has it extended to comparisons within a species to discover whether interspecific principles apply.

Here we examine intraspecific human osteocyte lacuna density (OCD). The speed at which bone is formed has much to do with the number of bone forming cells, the osteoblasts, that are available to lay down a mineralizable matrix. The rate of osteoblast proliferation establishes the rate at which these cells may become incorporated into lacunae within the bone matrix as osteocytes. Variability in the rate of incorporation among humans may provide metabolic information and help us to address intraspecific concomitants of the HHO within the species.

Evidence suggests OCD is negatively related to body mass in mammalian interspecific comparisons (Bromage et al., 2009; Mullender et al., 1996a). This is consistent with differences in life history strategy taken by mammals of varying body size and life history; small mammals having "fast" life histories manufacture their bone quickly for a relatively short period of time in deference to larger mammals that live "slow" life histories and produce their bone more slowly.

We thus have some understanding of the relationship between OCD and body mass among mammals of varying body size. But what of modern humans that have more body mass variability than most other mammals (Mutch et al., 2009)? This remarkable fact begs for an inquiry into the intraspecific relationship among humans and the mechanisms by which bone and body size are achieved. Given our understanding of why mammals reveal a negative relationship with body mass given their diverse life histories, we would expect that OCD among humans would be positive. We reason that if life history is held reasonably constant, then differences in body size among humans must reflect varying rates of osteoblast proliferation and osteocyte incorporation consistent with expectations of their HHOs, which vary from 6 to 12 days (Smith et al., 2007), with arithmetic means of 9 days in females and 8 days in males (Bromage et al., 2011a)

For instance, people with longer HHOs will be smaller, growing more slowly due to slower rates of bone cell proliferation than larger people that have shorter HHOs (the average size difference between males and females in all regional human populations agrees with the HHO sex difference).

2. Materials and methods

Twelve cadavers derived from sub-Saharan Africans (Malawi) of Bantu origin and known life history were selected from the gross anatomy program of the University of Malawi College of Medicine (UMCOM) (Table 1). UMCOM staff administered a questionnaire to the next of kin in which medical, social, economic, and life history information was sought. The medical history is particularly relevant to disease risk in Malawi. Social and economic history information relates to living conditions and employment. We also acquired common life history variables, such as age, height, and weight (mass). In addition, questions were developed to solicit information relating to autonomic function.

Midshaft femurs were obtained from each individual and processed for backscattered electron microscopy in the scanning electron microscope (BSE-SEM). Briefly, specimens, were subject to polymethylmethacrylate substitution and embedding. Each cured block was sawn through midshaft with a Buehler (Lake Bluff, IL) Isomet low-speed saw, hand ground through graded carbide papers to 1200 grit on a Buehler Handimet II and polished on a

[1] Biological periods longer than one day do not have an idiom associated with this phenomenon. We use the term "multidien", formed irregularly from the Latin *multis* 'many' + *dies* 'days'.

Table 1
Sample details and summary values are presented for 12 individuals of Bantu origin and known life history.
Tableau 1
Les details sur les échantillons et les valeurs résumées sont présentées pour 12 individus d'origine bantoue et dont l'histoire de vie est connue.

ID	Sex	Age	Weight (kg)	Height (m)	OCL Area (mm^2)	Total Bone Area (mm^2)	OC/mm^2
01 02	Female	50	68	1.6	4.25E-07	304.77	305
02 02	Male	40	60	1.5	2.36E-07	497.22	313
02 05	Male	42	64	1.72	5.63E-07	274.71	245
04 02	Male	17	48	1.1	6.4E-07	358.93	193
05 02	Male	22	52	1.9	2.47E-07	352.28	463
06 02	Male	38	82	1.78	4.55E-07	302.46	288
07 02	Female	28	58.2	1.64	4.14E-07	315.79	288
08 02	Male	42	78	1.5	4.97E-07	413.38	209
09 02	Male	26	82	1.75	3.54E-07	303.31	321
10 06	Male	32	58	1.3	3.56E-07	337.55	294
13 02	Male	40	80	1.65	3.81E-07	369.19	264
15 02	Female	35	60	1.2	3.93E-07	329.12	290

OCL: osteocyte lacuna.

Buehler Ecomet III to a finish provided by 1- μm diamond suspension.

BSE-SEM imaging was performed with a Zeiss EVO 50 SEM (Carl Zeiss Microscopy, LLC, Thornwood, NY) under the following conditions: 15 kV accelerating voltage, 600 pA current, 8.5 mm working distance, and 100 Pa pressure. Uniform beam conditions were obtained on a halogenated dimethacrylate, assigning the grey value of 5 to the mean of a monobromo standard and the grey value of 250 to a monoiodo standard (Boyde et al., 1995). Images were obtained that at most represent material density dependence to less than 1 μm depth. Whole femur gigapixel montages at 0.9793 μm/pixel resolution were obtained using Zeiss SmartStich software (Fig. 1). Monochrome 256 gray level images were processed by a program developed by our laboratory called "BSESEM", which employs the Matlab (Mathworks, Natick, MA) Image Processing Toolbox.

Lacunae have a characteristic roundness, perimeter, and area in BSE-SEM images that allow them to be identified and automatically enumerated relative to the detected bone area in all of the images processed (roundness = 0.35-maximum (1), based on the metric = 4 × pi × area/perimeter$\hat{2}$); (minimum-maximum lacuna area and perimeter = 10–69 pixels each). The BSESEM program has a variety of options that are manually entered when processing images obtained by BSE-SEM. The image is first transformed to a binary (grey levels 0 and 255). Then, "Clean", "Gaussian", and "Fill" filters are used to clean up the image by eliminating noise (small, isolated pixels) and separating objects (with shared borders) from one another. Once these options have been utilized, a "Finds Objects" option is employed to identify the number and area of all "objects" – groups of black pixels (grey level 0) – in the image, which includes osteocyte lacunae, vascular canals, and cracks. Total bone area is calculated by adding all pixels assigned to detected bone (grey level 255), lacunae, vascular canals, and cracks; cracks are necessary to add into total bone area because these features form as a result of bone shrinkage, not expansion. (Note: Total bone area was also calculated without including vascular canals, which did not have a material effect on the results, and which are not reported here). All values were exported to an Excel (Microsoft, Redmond, WA) spreadsheet, and all statistics were performed using IBM SPSS Statistics (v. 22.0; IBM Corporation, Armonk, New York). To evaluate osteocyte lacunae parameters in relation to measures of bone and body size, linear regressions were executed using the least squares model, reporting the Pearson product moment correlation coefficient (r), its statistical significance (P), the adjusted coefficient of determination (R^2), and the slope.

Table 2
Osteocyte lacunae density for three different bone packets is given for two individuals in the study sample. The number of osteons or interstitial bone packets is given in parentheses.
Tableau 2
La densité de lacunes d'ostéocyte pour trois paquets osseux différents est fournie pour deux des individus de l'échantillonnage étudié. Le nombre d'ostéones ou de paquets osseux interstitiels est donné entre parenthèses.

	Bright Osteons	Interstitial Bone	Dark Osteons
Individual			
01-02	334 (n = 97)	312 (n = 43)	276 (n = 123)
02-02	346 (n = 114)	310 (n = 70)	271 (n = 107)

To understand what variability in the OCD data may be attributable to ageing, three separate bone packets were measured. Bone packets representing relatively young age are assigned to the most densely mineralized osteons (bright in BSE-SEM), which have persisted longest in the skeleton. Interstitial bone is assigned to an intermediate age, as these packets represent a variety of bone mineral densities (bright to dark in BSE-SEM). Bone packets representing a relatively older age (i.e., near to the age of the individual at death) are assigned to the least densely mineralized osteons (dark in BSE-SEM), some of which were still infilling at the time of death. Image thresholding in Adobe Photoshop (CS5; San Jose, CA) was performed to separate osteons having grey levels 129 to 250 (bright) and 5-128 (dark). The two osteon classes and interstitial bone packets were digitally excised from the full size image by hand and montaged into images for processing by the BSESEM program described above (Table 2).

To obtain the HHO long period rhythm via the enamel repeat period, the teeth from the right lower jaw from four individuals in the study sample were also available and prepared similarly to the bone samples, excepting that each

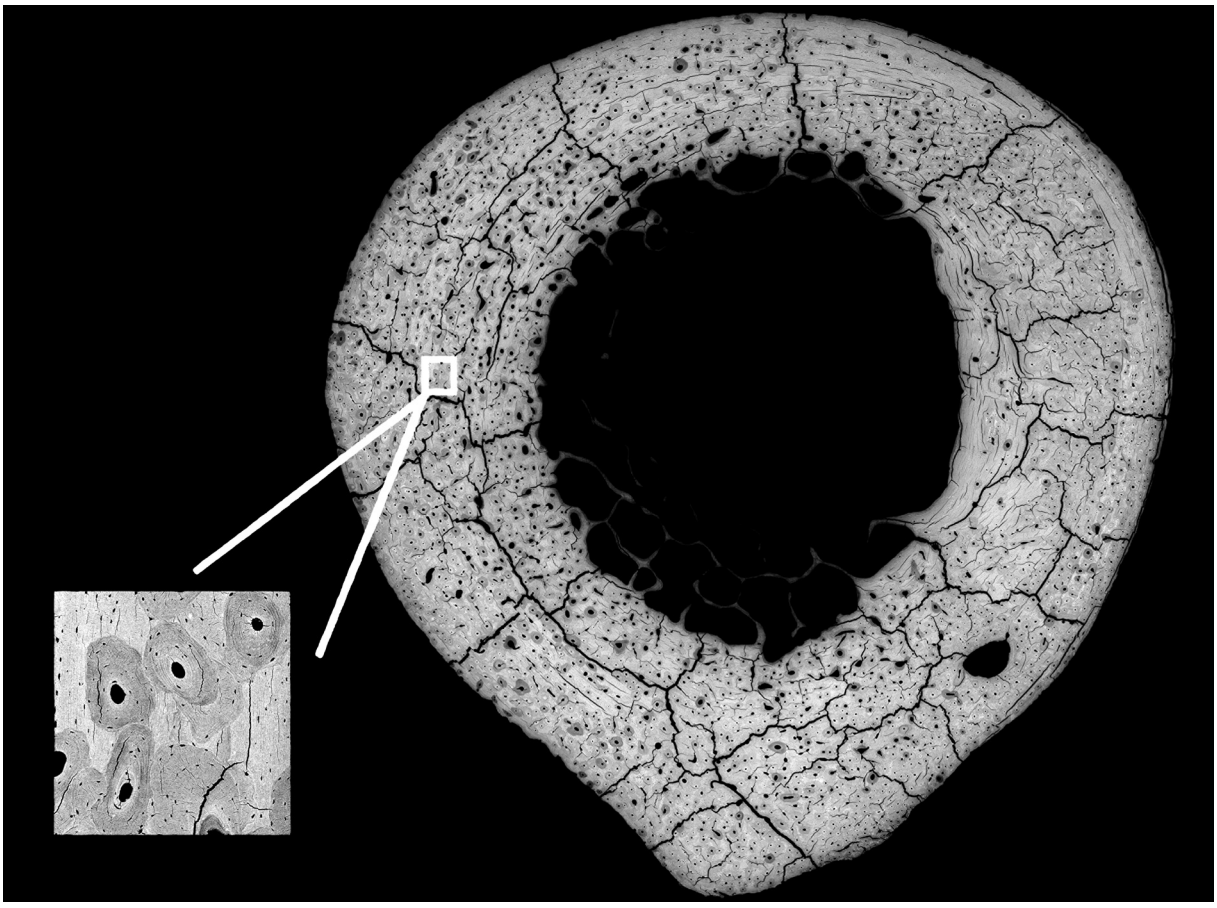

Fig. 1. Image of the midshaft femur cross section of individual 01 02 by backscattered electron microscopy in the scanning electron microscope. This density-dependent image renders bone in various levels of grey, while bone spaces are assigned to black. The detailed image at left shows several low density (dark) Haversian systems (osteons), each with a central vascular canal (black). The very small black spaces are osteocyte lacunae. Specimen width = 23.627 mm; detailed image FW = 619 μm.

Fig. 1. Image de section de la diaphyse fémorale de l'individu 01 02 en microscopie à électrons rétrodiffusés au microscope électronique à balayage. Cette image dépendant de la densité montre des niveaux variés de gris pour l'os, tandis que les espaces inter-osseux apparaissent en noir. Dans la zone encadrée à gauche, on peut observer plusieurs systèmes habersiens (foncés) de faible densité (ostéones), chacun présentant un canal vasculaire central (noir). Les très petits points noirs sont des lacunes d'ostéocyte. Largeur du spécimen = 23, 627 mm ; zone encadrée FW : 619 μm.

polished block was sawn using a Buehler Isomet low-speed saw to provide a ca. 100 μm histological thin section, which was then imaged by linearly polarized light using a Leica DM5000B microscope and a Leica PL Fluotar 40/0.70 objective lens (Leica Microsystems, Bannockburn, Ill., USA). The repeat period was obtained by counting the number of daily increments along enamel prisms between adjacent striae of Retzius.

3. Results

Sample details and summary values are presented in Table 1. Osteocyte parameters were measured over twelve whole human midshaft femur cross sections, which ranged in area from roughly 300–500 square millimeters. The number of osteocyte lacunae for entire adult femoral midshaft cross sections averaged about 100,000, and occupied a combined area that averaged about 0.7% of total bone area.

The average number of lacunae was standardized as the count per square millimeter of bone, in order to adjust for differences in femur size between individuals (Table 1). To determine if an increase in OCD was monotonic with lacuna area, as we suspected it might, Fig. 2 shows the relationship between OCD and osteocyte lacunae area (lacunae area/total bone area). The data points are gently sinusoidal in their distribution (dashed line), but the relationship is well described by a linear function ($r = 0.96$, $R^2 = 0.95$, $P < 0.01$). This arithmetic dependence between lacunae area and density suggests that both measures characterize a common aspect of bone conformation, and also indicate that individual lacunae remain constant in size with increasing OCD.

An assessment of the role of cell proliferation was calculated as a relationship between body height and the number of osteocyte lacunae per square millimeter. This relationship is described by the correlation $r = 0.56$, $R^2 = 0.25$, $P = 0.06$. This marginal, yet non-significant, result more or less met expectations. An examination of the results indicates that the tallest individuals have the greatest number of osteocyte lacunae, while the smallest

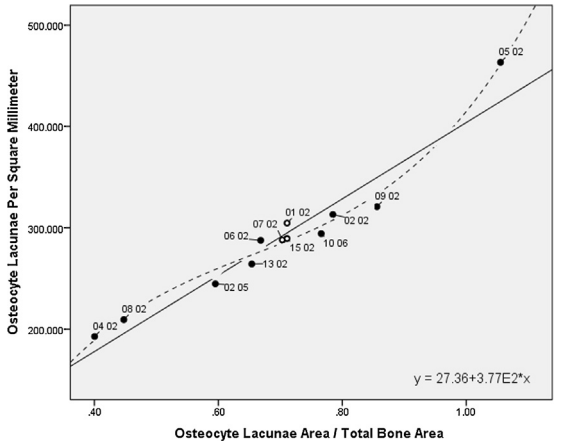

Fig. 2. Linear regression of osteocyte lacunae area/total bone area vs. the number of osteocyte lacunae per square millimeter. Osteocyte lacunae density is observed to increase monotonically with relative lacuna area. Females indicated by open circles, males by closed circles.
Fig. 2. Régression linéaire du rapport surface des lacunes d'ostéocyte sur surface totale de l'os en fonction du nombre de lacunes d'ostéocyte par millimètre carré. On observe une augmentation de type monotonique de la densité de lacunes d'ostéocyte avec la surface relative de lacunes. Les cercles blancs correspondent aux femelles, les cercles noirs aux mâles.

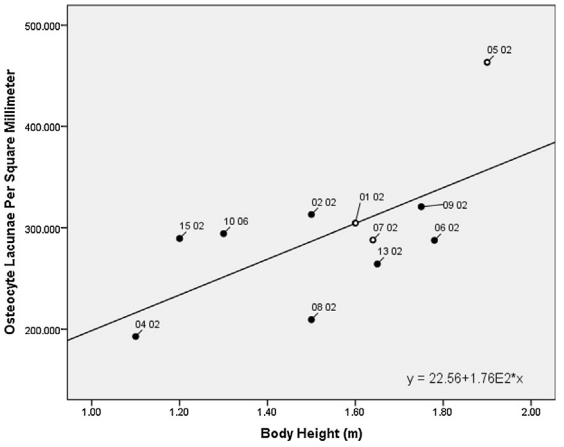

Fig. 3. Linear regression of body height vs. the number of osteocyte lacunae per square millimeter. This relationship demonstrates that osteocyte lacuna density scales positively with body height. Females indicated by open circles, males by closed circles.
Fig. 3. Régression linéaire de la taille en fonction du nombre de lacunes d'ostéocyte par millimètre carré. Les cercles blancs correspondent aux femelles et les cercles noirs aux mâles.

individuals have the fewest osteocyte lacunae. However, the questionnaires pertaining to the individuals sampled suggest that 02 05 is an outlier. Among the tallest in the sample, inspection showed his femoral bone cortices to be unusually thin (ca. 50% of average among others in the sample). Previously we discovered that this individual was one of two that deposited their bone during a period of drought (Bromage et al., 2011b), and of these two, only 02 05's life's history records reveal that they had experienced malnutrition. When this individual was removed from the analysis, the relationship between OCD per square millimeter and body height became significant and was

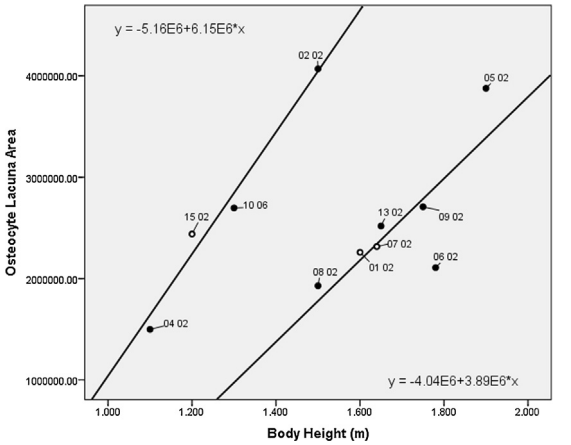

Fig. 4. Linear regressions of body height vs. absolute osteocyte lacunae area. This relationship reveals that, like for OCD, osteocyte lacuna area scales positively with body height. The data indicate the presence of two fundamental growth trajectories, one regression characteristic of relatively short people at left, and the other regression characterizing a relatively tall category of people at right. Females indicated by open circles, males by closed circles.
Fig. 4. Régressions linéaires de la taille en fonction de la surface absolue des lacunes d'ostéocyte. La formule révèle que, comme dans le cas de l'OCD, la surface des lacunes d'ostéocyte est en relation, de manière positive, avec la taille corporelle. Les données indiquent la présence de deux itinéraires fondamentaux pour la croissance, l'une qui est une régression caractéristique d'individus relativement petits, à gauche, et l'autre une régression caractérisant une catégorie d'individus relativement grands, à droite. Les cercles blancs correspondent aux femelles et les cercles noirs aux mâles.

described by the correlation $r = 0.63$, $R^2 = 0.34$, $P = 0.04$ (Fig. 3) (there was no significant relationship between OCD and weight). A test of the relationship between osteocyte lacuna area and body height including the whole data set did not reveal a significant result, but inspection of the scatterplot is revealing (Fig. 4). More so than of the relationship between body height and OCD (Fig. 3), the data sort into two distinct groups, one comprised of people 1.1–1.5 m tall, and the other of people 1.5–1.78 m tall, described by correlations of $r = 0.99$, $R^2 = 0.97$, $P = 0.01$ and $r = 0.79$, $R^2 = 0.56$, $P = 0.03$ respectively. This suggests that some fundamental difference in the growth program exists between these two height categories.

A preliminary assessment indicates that osteocyte density decreases with age (Table 2; Fig. 5). However, it appears that the effect of age has a normalizing influence on the whole-bone results. The OCDs of dark osteons were 17% and 22% lower than bright osteons for individuals 01-02 and 02-02 respectively. The decline is reasonably steady inasmuch as the mean OCD for all three bone packets as a percent difference from the OCD of bright osteons is 8% and 11% for individuals 01-02 and 02-02 respectively. These percent differences are nearly identical to the OCD of interstitial bone, being 7% and 10% respectively.

For several individuals in the study sample we have enamel specimens. Two of the shortest individuals in the sample, 10 06 and 15 02, have a repeat period of 8 days, while two of the tallest individuals, 06 02 and 09 02, have a repeat period of 7 days. Linear regressions were only performed for the purpose of examining the sign of the slope

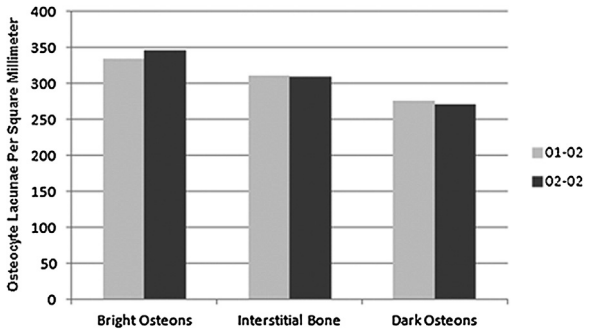

Fig. 5. Histogram of osteocyte lacunae density among bright osteons (highly mineralized bone formed when the individual was younger), dark osteons (poorly mineralized bone formed when the individual was older), and interstitial bone (both highly and poorly mineralized bone packets formed from different ages).
Fig. 5. Histogramme de la densité de lacunes d'ostéocyte parmi des ostéones brillantes (l'os intensément minéralisé s'est formé lorsque l'individu était jeune), des ostéones sombres (l'os faiblement minéralisé s'est formé lorsque l'individu était plus âgé) et de l'os interstitiel (paquets d'os faiblement ou très minéralisés, formés à différents âges).

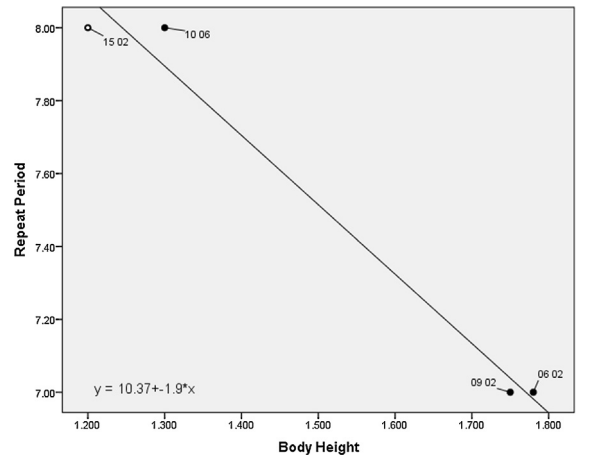

Fig. 6. Graph of enamel repeat period vs. height. While there is presently little data on repeat period, this provisional relationship suggests that repeat period scales negatively with height. Females indicated by open circles, males by closed circles.
Fig. 6. Graphe de période répétitive d'émail en fonction de la taille. Comme il n'existe pas beaucoup de données sur la période répétitive, il est suggéré, comme relation provisoire, que la période répétitive est à l'échelle de la taille, de manière négative. Les cercles blancs correspondent aux femelles et les cercles noirs aux mâles.

of repeat period vs. height (Fig. 6) and repeat period vs. weight (Fig. 7), which were both negative.

4. Discussion

Our BSE-SEM method of analysis is new, being designed to assess the total osteocyte lacuna population of – for all intents and purposes – an infinitely thin bone cross section. Because of this, we should first discuss what it is that we are actually measuring. Our 2D BSE-SEM technique may be perceived as a disadvantage, because what we calculate are relative numbers of lacunae, which is not a real measure of the rate of incorporation of osteoblasts as osteocytes during

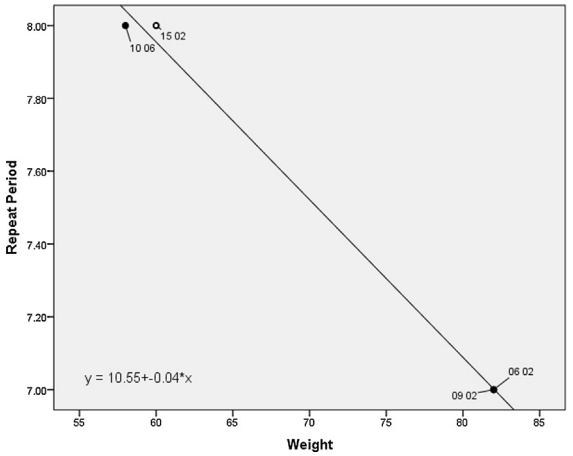

Fig. 7. Graph of enamel repeat period vs. weight. While there is presently little data on repeat period, this provisional relationship suggests that repeat period scales negatively with weight. Females indicated by open circles, males by closed circles.
Fig. 7. Graphe de période répétitive d'émail en fonction du poids. Comme il n'existe pas beaucoup de données sur la période répétitive, il est suggéré, comme relation provisoire, que la période répétitive est à l'échelle du poids, de manière négative. Les cercles blancs correspondent aux femelles et les cercles noirs aux mâles.

bone formation. The extremely thin imaging plane renders all possible cross sections through lacunae, artificially increasing their detected number over three dimensional (3D) techniques. However, while a 3D measurement may be preferred for having a better understanding of the rate of osteoblast incorporation, our 2D BSE-SEM protocol has some distinct advantages over present day 3D studies. The primary advantage is that entire bone cross sections may be evaluated. This results in very large numbers of detected lacunae that improve the statistics. Our light optics methods in 3D are relatively labor intensive, and like nano-CT analytical techniques, evaluate relatively small volumes (Bromage et al., 2009) (the main reason for developing the BSE-SEM method). The method is reasonably efficient in that while the image montaging of an adult human midshaft femur cross section (4–6 hrs beam time) and the OCD determinations (4–6 hrs desktop PC machine time) are presently time consuming, they are automated. We must acknowledge that age is also a factor affecting OCD in humans (Mullender et al., 1996b). In bone that has secondarily remodeled over many years, bone packets of all ages from childhood to adulthood are represented in the entire bone cross section (Table 2; Fig. 5). In the absence of controlling for age, evaluating the entire cross section will thus simply trend toward the most age-matched bone packets represented, which, in the preliminary case evaluated here, appears to trend toward the mean of OCD also represented by the OCD of interstitial bone. Because BSE-SEM renders a density dependent image, it may in future studies be possible to assess the effects of age more precisely by evaluating OCD according to the density histogram. That we obtain significant relationships between OCD and body size without controlling for age, suggests that within an entire cross section, the numerical density of osteocyte lacunae is powered by sufficient bone matrix formed at many ages.

Now to a discussion of our OCD research results. We calculated relative OCD from two dimensional (2D) BSE-SEM images of whole human midshaft femur cross sections. Acquired at sub-micron pixel resolution, these images have sufficient resolution to identify and measure 2D osteocyte lacuna parameters. The regression of osteocyte lacunae area/total bone area by osteocyte lacunae per square millimeter (Fig. 2) clearly shows that the tallest individual in the sample (05 02) has the greatest OCD (top right on the regression), and that the shortest individual in the sample (04 02) has the lowest OCD (bottom left of the regression). We confirmed the same by replacing osteocyte lacunae area/total bone area with body height on the X-axis, and finding a significant relationship between OCD and body height (Fig. 3). In deference to the negative relationship between OCD and body mass between species of mammals, the intraspecific relationship among human OCD and height is positive.

How is this explained? *Inter*specifically, life history is free to vary when we compare mammals of varying body sizes (constrained as it is phylogenetically, etc.; a discussion of mammalian historical contingencies may be found in Bromage et al., 2012). For instance, a comparison between the development of a small and large mammal illustrates that the evolution of large size is the outcome of reducing rates of cellular proliferation, as indicated by the negative OCD-mass relationship (Bromage et al., 2009; Mullender et al., 1996a), but growing at this reduced rate for longer periods of development time. This strategy must eventually overcome the mass "disadvantage" of slow growth. *Intra*specifically, however, life history and development time is reasonably controlled for. For instance, the growth durations and life histories of modern day people are roughly the same irrespective of their body size. Thus to manifest body size variability among individuals within a species, rates of cellular proliferation must increase at larger sizes. That is, a larger individual – having more or less the same duration of growth allotted to them as a smaller individual – would manifest a positive relationship between OCD and body size, increasing their rate of cellular proliferation in order to achieve larger size.

These inter- and intraspecific principles rationalize our OCD results with the scaling of metabolic rate. Although section thicknesses and bone elements varied between studies, the 2D OCD in the mouse is roughly 1300–1600 per square millimeter (5 μm section, ulna diaphysis) (Robling and Turner, 2002), whilst that in the dog is around 356–370 per square millimeter (20–30 μm section, humerus diaphysis) (Canè et al., 1982). (Note that these numbers are not readily comparable to the measurements made on the "infinitely thin" BSE-SEM images reported for humans in the present study). We know that with an interspecific comparison of mammals, whole-body basal metabolic rate (BMR) scales positively with body mass, while mass specific metabolic rates (SMR; a measure the respiration of tissues and organs) scale negatively with body mass, thus becoming more energy efficient with increased size (Schmidt-Nielsen, 1984). Using our example above, the BMR of a 20 gm mouse is 33.8 mL-O_2/hr while that of a 20 kg dog is 7200 mL-O_2/hr. However, the SMR of bone in these animals is about 0.3 mL-O_2/gm/hr and 0.03 mL-O_2/gm/hr respectively (Martin and Fuhrman, 1995). This factor of ten difference in the mass specific metabolic rate of bone is reflected in the interspecific negative scaling of OCD with body mass.

The intraspecific human data presented here differ from an interspecific comparison in that increased rates of cell proliferation are associated with larger people, leading to higher OCDs, not lower OCDs as one would find when comparing large to small mammals (when interspecific life histories are free to vary). The increase in OCD and the requisite increase in SMR and bone mass – afforded by the more highly proliferating cells in larger people – will contribute to a higher overall mass-dependent BMR. Interestingly, like the interspecific relationship, it appears that this also results in an increased efficiency of bone tissue SMR as bone mass increases in larger people. While there are most likely differences among mammalian taxonomic groups due to phylogenetic effects, the intraspecific increase in SMR and BMR at larger body sizes appears to be a function of building larger mass that is somewhat independent of life history. Inspection of the regressions of relatively short and tall people in Fig. 4 suggests that the SMR of bone is more energetically efficient at larger body sizes. Tall individuals have approximately the same range of variability in osteocyte lacuna area as smaller individuals, thus their height is carried in a more metabolically efficient state. But further, this efficiency extends to height categories even when height is the same. Short and tall height categories overlap at 1.5 m (Fig. 4), wherein we see that individual 08 02 on the tall trajectory has a dramatically lower osteocyte lacuna area than individual 02 02 on the short trajectory; individual 08 02 thus has a much lower SMR of bone.

Finally, we turn to the relationship between our OCD findings and the HHO. At present we only have four individuals for whom we have acquired HHO-generated repeat period values, thus we are unable to statistically assess repeat period against body size; regressions of repeat period with either height or weight have very high "*r*" and "$R^{2''}$ values and significant "*P*" values, but this is likely due to the extremely small sample size. In each of the regressions between repeat period and height or weight, the slope is negative (Figs. 6 and 7 respectively). According to theory, with increasing measures of body size, repeat period should diminish (Bromage et al., 2012) and indeed this is what we provisionally observe. Larger body size thus appears to be accomplished by shortening the repeat period, which refers to an accelerated HHO, that in turn relates to an increase in the rate of cellular proliferation.

Further work on individuals of known life history, for whom we can obtain both OCD and repeat period, are needed to bolster our understanding of metabolic signals in bone and tooth tissues. Meanwhile, hints about the nature of the mechanism(s) regulating bone metabolism and development are to be found in the relationship between body height and osteocyte lacuna area (Fig. 4). Of the four individuals for whom we have repeat period values, two 8-day individuals reside on the regression of relatively short people, while two 7-day individuals lie along the regression associated with relatively tall people. It is reasonable

to suggest that these two regressions represent the outcomes of fundamental processes steering growth along unique relatively long and short HHO-regulated trajectories to achieve adult body size. The variability in lacuna area among both body height groups is an indication that the HHO is only one moderating factor responsible for the rate of cell proliferation and achievement of body size. While body size groups may be HHO-determined, other factors must be recruited to regulate rates of cell proliferation in order to meet developmental targets in, say, height. Elucidation of these factors is presently the focus of chronobiological metabolomics experiments.

5. Conclusions

Sample sizes are low and presently marginal at best, thus the findings of our study are suggestive and need to be bolstered by future research. But overall, we conclude that osteocyte density is positively related to body height in humans. Taller humans, we suggest, achieve their body heights by growing more quickly and thus proliferating their bone cells more rapidly than shorter individuals, rendering a positive relationship between osteocyte density and body height. Given our understanding of comparative mammalian metabolism, our study also concludes that the mass specific metabolic rate of human bone follows an intraspecific pattern, increasing at larger body sizes and contributing to an overall higher basal metabolic rate. Finally, preliminary results indicate that the human enamel repeat period, together with its concomitant Havers-Halberg Oscillation, is a mechanism by which body size variability is manifest.

Acknowledgments

We thank Michel Laurin and Jorge Cubo for the opportunity to honor V. de Buffrénil, J. Castanet, H. Francillon-Vieillot, F. Meunier, A. de Ricqlès, and L. Zylberberg for a collective integrative body of work that has no match. The paper has benefited greatly from critical review by Chris Organ and two additional anonymous reviewers; the extent to which the paper reflects their reviews is our responsibility alone. Research support was provided by NSF award BCS-1062680 and the 2010 Max Planck Research Award to TGB, endowed by the German Federal Ministry of Education and Research to the Max Planck Society and the Alexander von Humboldt Foundation in respect of the Hard Tissue Research Program in Human Paleobiomics.

References

Boyde, A., Davy, K.W.M., Jones, S.J., 1995. Standards for mineral quantitation of human bone by analysis of backscattered electron images. Scanning 17, 6–7.

Bromage, T.G., Janal, M.N., 2014. The Havers-Halberg oscillation regulates primate tissue and organ masses across the life history continuum. Biol. J. Linnean Soc. 112, 649–656.

Bromage, T.G., et al., 2009. Lamellar bone is an incremental tissue reconciling enamel rhythms, body size, and organismal life history. Calcif Tissue Int. 84, 388–404.

Bromage, T.G., et al., 2011a. Enamel-calibrated lamellar bone reveals long period growth rate variability in humans. Cells Tissues Organs 194, 124–130.

Bromage, T.G., et al., 2011b. Signposts ahead: hard tissue signals on rue Armand de Ricqlès. C. R. Palevol 10, 499–507.

Bromage, T.G., et al., 2012. Primate enamel evinces long period biological timing and regulation of life history. J. Theor. Biol. 305, 131–144.

Canè, V., et al., 1982. Size and density of osteocfyte lacunae in different regions of long bones. Calcif. Tissue Int. 34, 558–563.

Martin, W., Fuhrman, F.A., 1995. The relationship between summated tissue respiration and metabolic rate in the mouse and dog. Physiol. Zool. 28, 18–34.

Mullender, M.G., et al., 1996a. Osteocyte density and histomorphometric parameters in cancellous bone of the proximal femur in five mammalian species. J. Orthop. Res. 14, 972–979.

Mullender, M.G., et al., 1996b. Osteocyte density changes in aging and osteoporosis. Bone 18, 109–113.

Mutch, D.M., et al., 2009. Metabolite profiling identifies candidate markers reflecting the clinical adaptations associated with Roux-en-Y gastric bypass surgery. PLoS ONE 4, e7905, http://dx.doi.org/10.1371/journal.pone.0007905.

Robling, A.G., Turner, C.H., 2002. Mechanotransduction in bone: genetic effects on mechanosensitivity in mice. Bone 31, 562–569.

Schmidt-Nielsen, K., 1984. Scaling: why is animal size so important? Cambridge Univ. Press, Cambridge, pp. 241.

Smith, T.M., et al., 2007. New perspectives on chimpanzee molar crown development. In: Bailey, S., Hublin, J.J. (Eds.), Dental palaeoanthropology. Springer, Berlin, pp. 177–192.